*This is the author's final version of the work, as accepted for publication following peer review but without the publisher's layout or pagination.
The definitive version is available at:
https://doi.org/10.1080/15376494.2023.2214553*

Optimisation of steel-reinforced wooden purlins

J.L. Osa[a,*], H. García[b], M. Zubizarreta[c], Z. Egiluz[d] and J. Cuadrado[d,**]

[a]*Mechanical Engineering Department, University of the Basque Country UPV/EHU, 29 Otaola Av., Eibar 20600, Spain*
[b]*Mechanical Engineering Department, University of the Basque Country UPV/EHU, 1 Europa Plaza, San Sebastian 20018, Spain*
[c]*Business Organization Department, University of the Basque Country UPV/EHU, 1 Europa Plaza, San Sebastian 20018, Spain*
[d]*Mechanical Engineering Department, University of the Basque Country UPV/EHU, 1 Ingeniero Torres Quevedo Plaza, Bilbao 48013, Spain*

j.osa@ehu.eus (J.L. Osa); arkaitz.garcia@ehu.eus (H. García)

ABSTRACT

A new structural typology of a Steel-Reinforced Wooden (SRW) purlin made of rectangular laminated wood and C-section type cold-formed steel is presented in this paper. The steel C-section profile is fitted onto the wooden purlin, so that both work together as a composite unit. Although the wooden sections are weaker and have a lower elastic modulus than the steel sections, the overall dimensions of the SRW purlins are no larger than the steel C-section purlin sizes. The SRW purlins also form lighter structures than either plain steel or wooden purlins and they therefore have lower CO_2 emissions. In addition, lighter purlins reduce the load on the main structure, which in turn reduces the material needed for the main structure of the building. So, reinforcement of the wooden purlin with steel sections within certain areas notably improved performance when compared with ordinary single-material purlins. The use of the SRW purlins can therefore improve the overall sustainability of a building. The improvements were analysed in terms of sustainability and lower weight, as a function of span length and design load. The behaviours of the single material purlins and the SRW purlin were also compared. Both material strength and deformation design criteria and their influence were studied using an analytical approach based on loading and span length. The simple, innovative, and reliable design procedure described in this study ensured compliance with all technical requirements. Moreover, the savings relating to material weight were evaluated, neutralizing the carbon footprint in all cases under analysis.

Keywords: Sustainability wooden structures steel structures purlins

1. Introduction

The construction sector, as one of the leading consumers of natural resources and energy, is responsible for the production of one-third of all greenhouse gas effects and 40 % of total energy consumption (1). The sector is responsible for consuming 30 % of the world's material resources, 12 % of all water resources, and for generating 30 % of all waste dumped in landfill sites. More recently, the sector has been at the forefront of several activities focused on the use of more durable, recyclable, reusable and naturally renewable materials, such as wood from sustainable forestry (2). It will take time to replace many standard construction materials. Although the development of techniques is now unstoppable, some lobbyists are resisting change, preferring instead to exploit immediate economic gain. Construction companies and public administrations should nevertheless listen to the demands of society, in order to ensure a decent future for coming generations (3; 4).

The sustainability of buildings and construction materials has been analysed in some models and some works have also been proposed to evaluate both the overall sustainability and the costs of conventional building structures (concrete, steel and wood). For example, Caruso *et al.* proposed a comparative evaluation methodology for the environmental sustainability of buildings based on a life-cycle assessment (5).

Wood has therefore become the reference sustainable material in construction today (6; 7; 8); government regulations now encourage the use of wooden structures among engineers and architects (9). Furthermore, some works have shown that a reduction in carbon emissions is achieved earlier in cities where wooden construction typologies are included in development planning (10; 11).

Wood is a well-known natural material. During its growth, the leaves of trees release oxygen through photosynthesis to produce solid fibrous materials (12). In other words, wood is a natural material whose growth is a consequence of chemico-biological reactions between sunlight and water. Trees therefore absorb and process ambient CO_2 (one of the main greenhouse gases), so as to create sugars that are converted into fibrous cellulose and lignin, and they also release smaller quantities of CO_2, *i.e.*, at night-time and when deciduous trees shed their leaves. An average tree is capable of absorbing and processing the equivalent of one CO_2 ton/m^3 through photosynthesis over a 100-year lifetime. Wood therefore has a negative carbon footprint and forests constitute the main atmospheric sinks of CO_2. When the life of a tree is over, wood becomes an attractive building material, both for structural and functional components, such as beams, columns, doors, and floors (13). In addition, wood can also be shredded into particles for the manufacture of agglomerate boards and pellet fuels (14; 15).

The environmental sustainability of wooden structures is good, even though they have design strength limitations. Multiple disciplinary studies should be encouraged to reduce the uncertainty that surrounds the design of wooden structures, and to gather further knowledge on the use of wood (16). In the book 'Tackle Climate Change - Use Wood', the expansion of sustainable material savings and forestry products is discussed (17). The authors proposed combinations of structural materials and feasible applications from a sustainable point of view, based on an optimal design of profile geometries. Hence, the idea of combining sections of steel and wood in the purlins that is proposed in this work.

In a preliminary study of the main structural components of a building (columns, beams and slabs) (18), the authors concluded that combining steel-wood profiles yielded disproportionate dimensions, in so far as a steel-wooden section that met the design requirements had to be much larger than a steel section. Thus, the use of the new concept in the main structural components was considered unfeasible. However, the concept of steel-wood composite materials could be applied to secondary structural components such as lightweight roof purlins, as the dimensional similarity between both materials is higher. The use of the SRW purlin is therefore studied in this work, an example of which is shown in Figure 1.

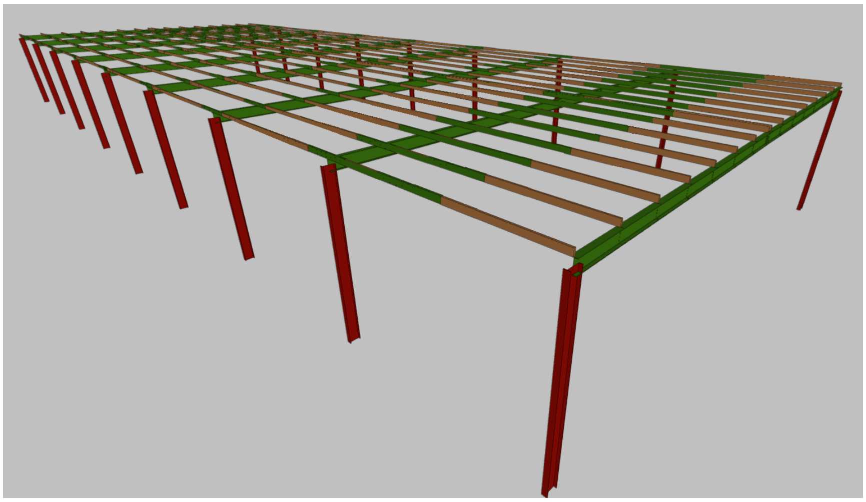

Figure 1: Example of an industrial pavilion where the structure of the lightweight roof is composed of SRW purlins: wood (orange) spans the entire length, whereas the steel C-section (green) reinforces the areas that withstand the highest loading.

New attempts to improve purlins have been proposed in the literature. The traditional wooden purlin is still of interest to researchers who have applied new test methods and designs to gain further knowledge of wooden materials and to improve structural reliability (19). Cold-formed (CF) steel profiles, the most widely used purlins, have also updated current design procedures (20). Prefabricated concrete purlins have been proposed as a substitute for steel profiles (21), although they are subject to potential shear cracking that can lead to structural failure. Traditional structural materials have also been compared from the point of view of sustainability throughout their service life (22). As structural elements, purlins are designed according to the respective technical regulation, e.g. the Spanish Technical Building Code (23). These regulations are usually based on analytical methods of beam design, which include a hidden safety factor. The review of Sayyad *et al.* (24) compile up to 300 articles on modelling and analysis of sandwich beams using elasticity theory, analytical methods, and numerical methods based on shear deformation theories. The state-of-the-art computational modelling (25) shares with the classical transformed section method (26) the ability to model the mechanical behaviour of heterogeneous beams. The experimental measurement of surface stresses on sandwich beams deserves special attention (27). This work has used the transformed section method, besides its adequacy with the problem nature, because technical regulations are based on analytical methods indeed. This method assumes an isotropic behaviour of materials, a common simplification in the construction engineering field.

This work continues the study of Garcia *et al.* (28) where a hybrid Steel-Wooden Purlin (SWP) consisting of wooden sections subject to lower stress levels was inserted into a steel C-section profile. The purlin was formed of alternate wooden and steel sections, with both materials overlapping at the joints. In this way, the wood section that was required was considerably reduced, in comparison with a wooden purlin of the same length, and under the same loading scheme. The SRW purlin, a simpler form of the SWP concept, is proposed in this study: the section remains constant throughout the length of the purlin, the wooden purlin extends throughout the whole length, while the steel C-section profile is only inserted around the wooden purlin in the areas under higher mechanical stress that are subject to greater deformation (Fig. 2). This configuration reduces both the required wood section and the use of steel. In turn, the SRW purlin responds to the increasingly high sustainability standards that are demanded by society. The bond between wood and steel is strong and rigid, guaranteeing continuity to withstand stress and deformation. Moreover, no dirt can accumulate within the closed geometry of the new design, which could foreseeably reduce maintenance work.

Figure 2: An example of an SRW purlin: C120.40 (laminated timber embedded in a steel profile).

The purlin was optimised using the transformed section method, minimizing the quantity of wood and steel in accordance with the load and span length. Then, the reduction in weight achieved by the new SRW purlin typology was studied in comparison with a single-material purlin (either wood or steel). Finally, the improvements to the sustainability of these purlins were analysed following the criteria set by Cuadrado *et al.* (29).

2. Materials and methodology

The characteristics of the materials, the SRW purlin proposed in this work, and the methodology followed for its development are all described in this section.

2.1. Scope of the Project

Today, the distance between frames in steel and wooden structures is similar: these distances are generally neither shorter than 6.5 m, nor longer than 8.5 m. Roof inclinations vary from 0 % (flat roofs) to a maximum of 35 %. Besides, the separation between purlins, typically between 1.25 and 2.5 m, depends on the stiffness of the roofing component.

The load of the roofing material varies from 90 kg/m^2 for simple plates to almost 200 N/m^2 for sandwich panels. Across most geographical regions of Spain, the design loads of lightweight roofs are based on maximum foreseeable levels of snowfall (700 N/m^2) and wind force (1000 N/m^2) (23). An overload of 400 N/m^2 was considered for areas with little or no snow and no wind loads (23).

Having looked at the usual features of purlins, the scope of this work was limited to purlins with spans of 6.5 m, 7.5 m, and 8.5 m, applied to lightweight flat roofs with 0 % slope, and loads between 800 N/m^2 and 3600 N/m^2 that were increased in steps of 400 N/m^2.

Table 1
Mechanical properties of laminated wood (GL36h) and steel (S235JR). The data of the laminated wood corresponds to the 5th percentile.

	Admissible stress σ_{adm} (MPa)	Modulus of elasticity E (GPa)	Density ρ (kg/m^3)
Laminated wood	36 (parallel to the grain)	11.6 (parallel to the grain)	410
Steel	235	200	7850

2.2. Materials and profiles

IPE laminated and cold-formed C or Z profiles are the most widely used metallic purlins for lightweight roofs. Both have similar characteristics (30). Cold-formed C profiles were chosen for the proposed SRW purlin typology: their open geometry fit perfectly on wooden rectangular purlins, forming a composite materials that works together to ensure the continuity of the beam.

The calculation method for the SRW purlins was applied to a glue laminated *Pinus radiata* timber, generally known as glulam, regardless of the type of timber in use. The methodology can be easily adapted to any type of wood. In particular, GL36h grade glulam was chosen where "36" refers to the bending resistance in MPa. S235 steel was used to reinforce the wooden beams. Table 1 compiles the mechanical properties of the glulam and the steel. The differences are evident: the steel is 6.5 times more resistant than the wood and 17 times stiffer. However, as wood is 17 times lighter than steel, its strength/weight ratio is nearly three times greater.

Besides its mechanical properties, stress and deflection depend closely on the area moment of inertia (I_z) of the profile. The proposed SRW purlin has a rectangular wooden beam reinforced with steel in certain sections to form the composite purlin (31). A perfect bonding between both materials with no loose spaces was considered in their design, which entails continuity in the deformation diagram of the section, but not in the stress distribution diagram of the section, which depends on the elastic module. The transformed section method was used, under the assumption that the section was formed of a single material (26; 31). In this study, the whole purlin was assumed to be made of wood. Table 2 introduces the sections used in this work. The C profiles and wooden beams were assumed to have sharply rounded edges.

The C profile dimensions are specified in UNE 36573:1979 (32). Each C profile size is available in two or three t thicknesses. The thinnest C profile of each size was selected, as the purpose of the C profile was to strengthen the wooden purlin. There must be a strong bonding between wood and steel: narrow tolerances must be assured to avoid looseness, but at the same time, the wood must be able to enter into the steel profile. The openness of the C profile helps to place the steel profile on the wooden purlin. Once the steel is laid on the wood, the two profiles are screwed together.

2.3. The mechanical behaviour of a purlin

A purlin is a continuous beam. The bending moment provokes normal stresses and deformations at the deflection point; the arrow-shape displacement of the beam arises from the sum of all deformations. Nonnast (33) proved that there were no noticeable changes in shear forces, bending moments, and deformations throughout the length of intermediate spans of continuous beams with four or more spans. Thus, accuracy could be maintained when considering only four spans in the calculus of the maximum bending moment and deflection in a continuous beam and the results were useful for structures with over four spans. Applying symmetry, the functions of the shear forces $V(x)$ and bending moments $M(x)$ of a four-span continuous beam according to the position x are introduced in Table 3.

The diagram of the internal forces of a four-span continuous beam (33) is shown in Figure 3. The bending moment is zero at the supports of the beam ends. Rather than at those supports, the maximum bending moments are adjacent to them and are 40 % higher than at the middle. In-between the spans, the bending moments are higher at the side spans (40 % smaller than the maximum) than at the intermediate ones (70% smaller). The bending moment, M, depends on the distributed load, q, and the square of the span length, L, in all cases. In terms of purlin strength, the reinforcement of high bending moment areas with the C profile leads to a direct reduction of the section of the wooden purlin, lightening the areas with bare wooden sections that support less load. In terms of deformation, the two ends of the purlin are the critical regions, because the purlin is free to rotate on the end supports. The deflection in lateral spans is three times

Table 2
Average values (SRW profile dimensions) (h, b, c, t), surface (A), area moment of inertia (I_z) and mass centre positions (d). The transformed section is assumed to be wooden (I_z^{SRW}).

	C140.2.0	C160.2.0	C180.2.0	C200.2.0	C225.2.5	C250.2.5	C275.2.5	C300.2.5
h (mm)	140	160	180	200	225	250	275	300
b (mm)	50	60	60	60	80	80	80	80
c (mm)	20	20	20	20	25	25	25	25
t (mm)	2	2	2	2	2.5	2.5	2.5	2.5
A (mm^2)	532	612	652	692	1050	1110	1170	1230
I_z^C (mm^4)	$1.6{\cdot}10^6$	$2.4{\cdot}10^6$	$3.2{\cdot}10^6$	$4.1{\cdot}10^6$	$8.1{\cdot}10^6$	$10.3{\cdot}10^6$	$12.9{\cdot}10^6$	$15.9{\cdot}10^6$
I_z^W (mm^4)	$11.4{\cdot}10^6$	$20.5{\cdot}10^6$	$29.2{\cdot}10^6$	$40.0{\cdot}10^6$	$75.9{\cdot}10^6$	$104.2{\cdot}10^6$	$138.6{\cdot}10^6$	$180{\cdot}10^6$
I_z^{SRW} (mm^4)	$37.2{\cdot}10^6$	$60.1{\cdot}10^6$	$81.4{\cdot}10^6$	$107.1{\cdot}10^6$	$209.2{\cdot}10^6$	$274.5{\cdot}10^6$	$351.9{\cdot}10^6$	$442.9{\cdot}10^6$
d^C (mm)	16	18.6	17.5	16.6	23.8	22.5	21.4	20.4
d (mm)	20.48	24.63	24.23	23.92	32.63	32.20	31.85	31.55
EI_z^C (Nmm^2)	$3.3{\cdot}10^{18}$	$5.0{\cdot}10^{18}$	$6.6{\cdot}10^{18}$	$8.5{\cdot}10^{18}$	$16.9{\cdot}10^{18}$	$21.6{\cdot}10^{18}$	$27.1{\cdot}10^{18}$	$33.4{\cdot}10^{18}$
EI_z^W (Nmm^2)	$1.5{\cdot}10^{18}$	$2.6{\cdot}10^{18}$	$3.7{\cdot}10^{18}$	$5.1{\cdot}10^{18}$	$9.6{\cdot}10^{18}$	$13.2{\cdot}10^{18}$	$17.6{\cdot}10^{18}$	$22.9{\cdot}10^{18}$
EI_z^{SRW} (Nmm^2)	$4.7{\cdot}1^{18}$	$7.6{\cdot}10^{18}$	$10.3{\cdot}10^{18}$	$13.6{\cdot}10^{18}$	$26.6{\cdot}10^{18}$	$34.9{\cdot}10^{18}$	$44.7{\cdot}10^{18}$	$56.3{\cdot}10^{18}$

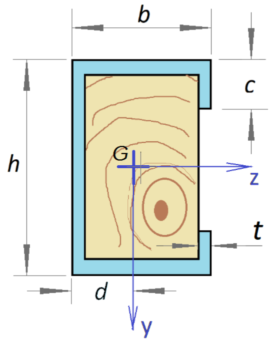

Table 3
The functions of a four-span grid to position x.

1st span $x \in (0, L)$	**2nd span** $x \in (L, 2L)$
$V_{AB}(x) = A - qx = 0.393qL - qx$	$V_B C(x) = B' - qx = 0.536qL - qx$
$M_{AB}(x) = Ax - q\frac{x^2}{2} = 0.393qLx - q\frac{x^2}{2}$	$M_{BC}(x) = B'x - q\frac{x^2}{2} + k = 0.536qLx - q\frac{x^2}{2} + 1.036$

larger than at the intermediate spans. However, a reinforcement in the end areas would not stiffen the purlin. In turn, the strengthening of the adjacent support reduces the deflection on the lateral span, as the purlin is a continuous beam.

According to the current Spanish Technical Building Code (23), purlins must fulfil two conditions: they must not exceed a material strength of ($\sigma_{max} \geq \sigma_{adm}$) and a deflection ratio 300 times smaller than the span length ($y \leq L/300$).

Figure 4 introduces the four-span configuration used in the SRW purlin that benefits from a symmetrical design. The lengths of the steel-wood combined parts are defined by the variables a, b, and c. In this study, the aim was to define the steel-wood timber configuration that could minimize both the wood profile size and the weight of steel and that was compliant with the maximum stress and deflection design requirements according to the span length, L, and the uniformly distributed load, q. The maximum stress and deflection of each configuration was a discrete calculation, *i.e.*, the values of lengths a, b, and c, rather than continuous values, were multiples of the d_p discretisation factor. As commented earlier, stress and deflection conditions are similar in purlins with more than four spans. Thus, parameter c can be applied in intermediate supports in those cases. Scilab 6.0.2 software was used for the numerical analysis.

The size of the discretisation factor, d_p, determines the accuracy of lengths a, b, and c, and the number of combinations to be studied. The sensitivity of d_p (0.1, 0.2, 0.3, 0.4, 0.5, and 0.6 m) was analysed, to determine the optimal a, b, and c parameters on a given purlin length ($L = 6.5$ m), under eight q loads (800, 1200, 1600, 2000, 2400, 2800, 3200, and 3600 N/m) for each d_p. The reference discretisation length was set at $d_p = 0.1$ m (a0.1, b0.1, c0.1), which provided the most accurate results. Assuming that the a-b-c optimal combination was only one, the Mean Squared Error (MSE) was estimated for each size of d_p with regard to the sum of squares calculated with n_q load cases

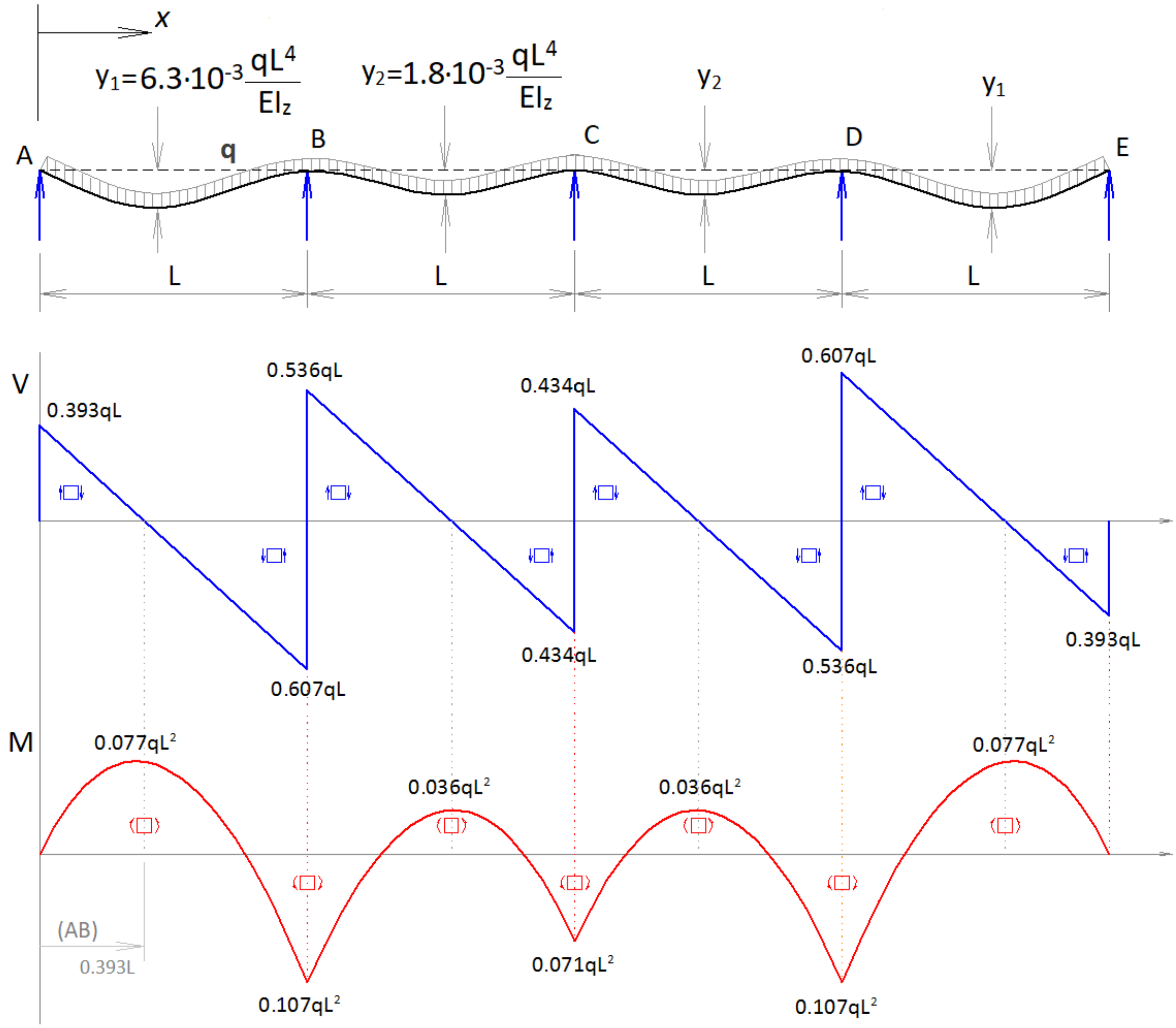

Figure 3: Diagram of the internal forces of a four-span continuous beam under a uniformly distributed load, *q*, throughout its length: shear force, *V*, and bending moment, *M*, diagrams (adapted from (33)).

$$\text{MSE} = \sqrt{\frac{\sum_{q=800}^{3600}(a_{dp}-a_{0.1})^2}{n_q}} + \sqrt{\frac{\sum_{q=800}^{3600}(b_{dp}-b_{0.1})^2}{n_q}} + \sqrt{\frac{\sum_{q=800}^{3600}(c_{dp}-c_{0.1})^2}{n_q}}$$

The stress was calculated with Navier's Formula (31), paying special attention to two points: the second support (B) and the point of maximum stress in the first span ($x_{AB} = 0.393L$). The highest bending moment was observed at the second support where the wooden purlin was reinforced with the C-section. However, the purlin was not reinforced in the first span at position x_{AB}. Taking the wood as a reference ($n = E_c/E_w$), the stresses were calculated by means of the transformed section method:

Wood: $\sigma_w = \frac{My}{I_{LN}}$ Steel C-section: $\sigma_c = n\sigma_w = \frac{E_c}{E_w}\frac{My}{I_z^{SRW}}$

The deflections were calculated by integrating the bending moment functions of Table 3 twice and by applying the conditions for continuity. Both the slope $\theta(x)$ and the deflection $y(x)$ with regard to the initial position are compiled in Table 4.

These steps were followed in the procedure for calculating the optimal profile size and reinforcement lengths for each load, q, and span length, L. First, the required section was calculated considering that it was completely made of

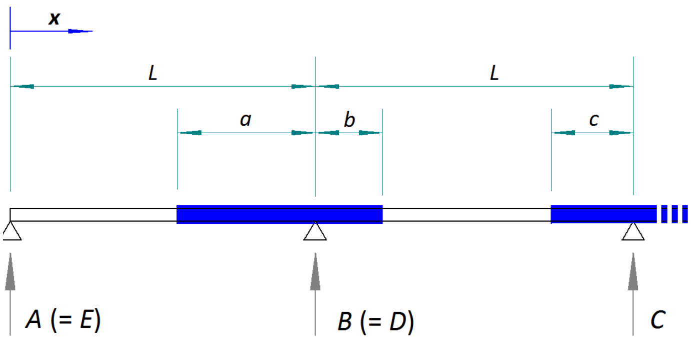

Figure 4: The four-span beam used in the design of SRW purlins. As both the beam and the loads are symmetrical, only the first two spans are defined in the figure. The steel-wood profile (in blue) is formed of lengths *a*, *b*, and *c*.

Table 4
Slope $\theta(x)$ and deflection $y(x)$ functions for the purlin in position *x*, obtained by integration of the bending moment $M(x)$ functions (Table 3).

Slope $\theta(x)$ by integration of $M(x)$ **1st span,** $x \in (0, L)$	**2nd span,** $x \in (L, 2L)$
$\theta(0,a) = \frac{1}{E_w I_w}\left(A\frac{x^2}{2} - q\frac{x^3}{6} + k_1\right) =$ $= \frac{1}{E_w I_w}\left(0.3929qL\frac{x^2}{2} - q\frac{x^3}{6} + k_1\right)$	$\theta(L, L+b) = \frac{H}{E_w I_w}\left(B'\frac{x^2}{2} - q\frac{x^3}{6} + k_3\right) =$ $= \frac{0.3071}{E_w I_w}\left(0.5357qL\frac{x^2}{2} - q\frac{x^3}{6} + k_3\right)$ $\theta(L+b, 2L-c) = \frac{1}{E_w I_w}\left(B'\frac{x^2}{2} - q\frac{x^3}{6} + k_4\right) =$ $= \frac{1}{E_w I_w}\left(0.5357qL\frac{x^2}{2} - q\frac{x^3}{6} + k_4\right)$
$\theta(a, L) = \frac{H}{E_w I_w}\left(A\frac{x^2}{2} - q\frac{x^3}{6} + k_2\right) =$ $\frac{0.3071}{E_w I_w}\left(0.3929qL\frac{x^2}{2} - q\frac{x^3}{6} + k_2\right)$	$\theta(2L-c, 2L) = \frac{H}{E_w I_w}\left(B'\frac{x^2}{2} - q\frac{x^3}{6} + k_5\right) =$ $= \frac{0.3071}{E_w I_w}\left(0.5357qL\frac{x^2}{2} - q\frac{x^3}{6} + k_5\right)$
Deflection $y(x)$ by integration of $\theta(x)$ 1^{st} **span,** $x \in (0, L)$	2^{nd} **span,** $x \in (L, 2L)$
$y(0,a) = \frac{1}{E_w I_w}\left(A\frac{x^3}{6} - q\frac{x^4}{24} + k_1 x + k_6\right) =$ $= \frac{1}{E_w I_w}\left(0.393qL\frac{x^3}{6} - q\frac{x^4}{24} + k_1 x + k_6\right)$	$y(L, L+b) = \frac{H}{E_w I_w}\left(B'\frac{x^3}{6} - q\frac{x^4}{24} + k_3 x + k_8\right) =$ $= \frac{0.307}{E_w I_w}\left(0.536qL\frac{x^3}{6} - q\frac{x^4}{24} + k_3 x + k_8\right)$ $y(L+b, 2L-c) = \frac{1}{E_w I_w}\left(B'\frac{x^3}{6} - q\frac{x^4}{24} + k_4 x + k_9\right) =$ $= \frac{1}{E_w I_w}\left(0.536qL\frac{x^3}{6} - q\frac{x^4}{24} + k_4 x + k_9\right)$
$y(a, L) = \frac{H}{E_w I_w}\left(A\frac{x^3}{6} - q\frac{x^4}{24} + k_2 x + k_7\right) =$ $= \frac{0.307}{E_w I_w}\left(0.393qL\frac{x^3}{6} - q\frac{x^4}{24} + k_2 x + k_7\right)$	$y(2L-c, 2L) = \frac{H}{E_w I_w}\left(B'\frac{x^3}{6} - q\frac{x^4}{24} + k_5 x + k_1 0\right) =$ $= \frac{0.307}{E_w I_w}\left(0.536qL\frac{x^3}{6} - q\frac{x^4}{24} + k_5 x + k_1 0\right)$
Conditions for continuity	
$\theta(a), \theta(L), \theta(L+b), \theta(2L-c), \theta(2L) = 0$ $y(0) = 0, y(a), y(L) = 0, y(L+b), y(L-c), y(2L) = 0$	

a single material: (1) C-section steel and (2) wood. The optimal dimensions of the SRW purlin were between these results. Then, beginning with a SRW purlin with the C-section dimensions, (3) the maximum stresses and (4) deflection were calculated for all possible combinations of parameters *a*, *b*, and *c* (Fig. 4), according to d_p. Parameters *a*, *b*, and *c* were multiples of the discretization length, d_p, and their values were limited, so that the SRW purlin was feasible: $a_{max} = L/2$, $b_{max} = L/3$ and $c_{max} = L/3$. (5) The optimal solution was the one that required the minimum amount of steel. Finally, the results of all the cases are compiled in the table, to form a design guide that could assist with any structured implementation of an SRW purlin. In addition, (6) the equivalent CO_2 value of the new solution was estimated.

3. Results and discussion

3.1. Sensitivity analysis of the discretisation length

The sensitivity of the discretization length, d_p, was studied in a $L = 6.5$ m purlin for $n_q = 8$ cases of q loading from 800 N/m to 3600 N/m. Figure 5 shows a graph of the mean squared error for parameters *a, b* and *c* or SRW purlin in relation to d_p, in other words, the required length of profile C. Taking $d_p = 0.1$ m as a reference, the graph shows the linear variation of MSE in relation to d_p, except when $d_p = 0.6$ m. As the results are discrete, the reduction indicates that the optimal result was fortuitously closer to the multiples of 0.6; had more cases been examined, then the error would have shown an upward trend (28). Knowing that the average steel length was 4.75 m, for (28) = 0.2 m, the relative error was 4.3 %, less than 5 %. Thus, $d_p = 0.2$ m was chosen for the design of SRW purlins, to ensure an accuracy level of 5 % when designing the SRW purlins and to maintain the balance between accuracy and minimum computing cost.

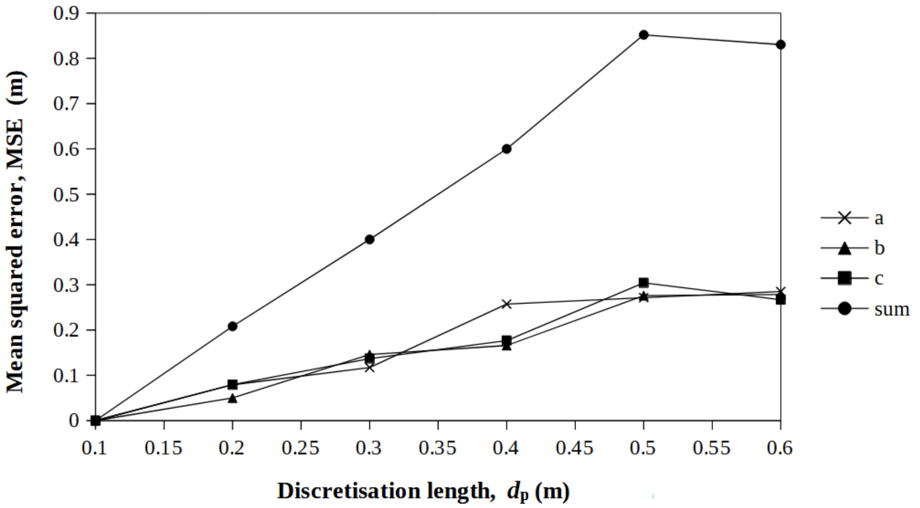

Figure 5: MSE parameters *a*, *b*, and *c*, according to d_p for a $L = 6.5$ m purlin.

3.2. SRW purlin optimisation

Once d_p had been set, all the possible purlin configurations for the parameters *a*, *b*, and *c*, were calculated for the four-span purlin shown in Figure 4. Table 5 presents the required profile sizes for purlins with spans of 6.5 m, 7.5 m, and 8.5 m, according to the two design criteria: admissible stress and deflection. First, the dimensions of the purlin for both cases were calculated considering the purlins manufactured out of steel (C), wood (W), and steel-reinforced wood (SRW). Then, taking these results as boundaries, all the combinations of reinforcement lengths (*a, b, c*) were discretely calculated according to d_p. The combinations that required a minimum weight of steel and the smallest wooden profile were the optimal SRW purlin for each span length and load case.

Given the strength and deflection criteria, it was remarkable that in all cases the deflection ratio of *L*/300 was more demanding than the strength, which required a smaller profile size. Analysing the results of the non-optimised purlins that maintained the section (W, C and SRW), the SRW profiles generally met the requirements with the smallest section size, smaller than the C-section steel. These encouraging results were the outcome of a higher bending stiffness EI_z (see Table 2). Taking the EI_z^W of wood as a reference, the EI_z^C of steel was 46 - 125 % higher and the EI_z^{SRW} of SRW, 145 - 225 % higher (Fig. 6). The bending stiffness differences were greater in small profile sizes. There was also a significant jump between a size of 200 and a size of 225: besides the width (from 60 mm to 80 mm), the C-section was also 0.5 mm thicker.

However, the use of SRW over the entire length is a waste of material. In some areas the capabilities of the profile are underused, as they could withstand higher stresses. The profile sizes obtained after optimization were in many cases even between the SRW and the C-sections. The optimised results, besides being the smallest sum of variables *a*, *b*, and *c,* also fulfilled their set limits ($a_{max} = L/2$, $b_{max} = L/3$ and $c_{max} = L/3$). In some cases, a_{max} is a condition

Table 5
Required profile size for $L = 6.5$ m, 7.5 m and 8.5 m span purlins made of wood (W), steel (C), and steel-reinforced wood (SRW), with regard to the load, q, for two design criteria: strength (maximum bending moment M_{max} and admissible stress σ_{max}), deflection ($y < L/300$), and dimensions of the optimised SRW purlin: profile size and a, b, and c parameters. The cells in exceeded the capabilities of the maximum profile size set out in the study.

	Load	**Strength criterion (M_{max} and σ_{adm})**					**Deflection criterion ($y_{max} < L/300$)**			**Optimised SRW**			
	q (N/m)	M^{B}_{max} (Nm)	M^{AB}_{max} (Nm)	Steel C	Wood W	Entire SRW	Steel C	Wood W	Entire SRW	Optimum SRW	a (m)	b (m)	c (m)
$L = 6.5$ m	**800**	3617	2603	C140.2.0	W140.50	(e)SRW140	C160.2.0	W200.60	(e)SRW140	SRW160	1.8	1.4	1
	1200	5425	3904	C140.2.0	W140.50	(e)SRW140	C180.2.0	W225.80	(e)SRW160	SRW180	1.4	1.6	1.2
	1600	7233	5205	C160.2.0	W160.60	(e)SRW140	C200.2.0	W225.80	(e)SRW180	SRW180	2.2	1.6	1.2
	2000	9042	6507	C200.2.0	W160.60	(e)SRW160	C225.2.5	W250.80	(e)SRW200	SRW200	2.6	1.8	1.4
	2400	10850	7808	C225.2.5	W180.60	(e)SRW160	C225.2.5	W250.80	(e)SRW200	SRW225	1.8	1.4	1.2
	2800	12658	9109	C225.2.5	W180.60	(e)SRW180	C225.2.5	W275.80	(e)SRW225	SRW225	2.2	1.6	1.2
	3200	14466	10410	C225.2.5	W200.60	(e)SRW200	C225.2.5	W275.80	(e)SRW225	SRW225	2.8	1.8	1.4
	3600	16275	11712	C225.2.5	W200.60	(e)SRW225	C250.2.5	W300.80	(e)SRW225	SRW250	1.8	1.6	1.2
$L = 7.5$ m	**800**	4815	3465	C140.2.0	W140.40	(e)SRW140	C180.2.0	W225.80	(e)SRW160	SRW180	1.8	1.6	1.2
	1200	7223	5198	C160.2.0	W160.60	(e)SRW140	C225.2.5	W225.80	(e)SRW180	SRW200	2.2	1.8	1.4
	1600	9630	6930	C200.2.0	W160.60	(e)SRW160	C225.2.5	W250.80	(e)SRW200	SRW225	2.2	2	1.4
	2000	12038	8663	C225.2.5	W180.60	(e)SRW180	C225.2.5	W275.80	(e)SRW225	SRW225	2.8	2.2	1.6
	2400	14445	10395	C225.2.5	W200.60	(e)SRW200	C250.2.5	W300.80	(e)SRW225	SRW250	2	1.4	1.2
	2800	16853	12128	C225.2.5	W225.80	(e)SRW225	C275.2.5	W300.80	(e)SRW225	SRW250	2.4	1.8	1.4
	3200	19260	13860	C250.2.5	W225.80	(e)SRW225	C275.2.5	-	(e)SRW225	SRW275	3	2	1.6
	3600	21668	15593	C275.2.5	W225.80	(e)SRW225	C300.2.5	-	(e)SRW250	SRW300	2.2	1.6	1.2
$L = 8.5$ m	**800**	6185	4451	C160.2.0	W140.40	(e)SRW140	C225.2.5	W225.80	(e)SRW180	SRW200	2.8	2.2	1.4
	1200	9277	6676	C200.2.0	W160.60	(e)SRW160	C225.2.5	W275.80	(e)SRW225	SRW225	2.4	2	1.4
	1600	12369	8901	C225.2.5	W180.60	(e)SRW180	C250.2.5	W300.80	(e)SRW225	SRW225	3	2.2	1.6
	2000	15462	11127	C225.2.5	W200.60	(e)SRW200	C275.2.5	-	(e)SRW225	SRW250	2.4	2.2	1.4
	2400	18554	13352	C250.2.5	W225.80	(e)SRW225	C300.2.5	-	(e)SRW250	SRW250	2.8	2.2	1.8
	2800	21646	15577	C275.2.5	W225.80	(e)SRW225	C300.2.5	-	(e)SRW250	SRW275	2.8	2	1.4
	3200	24738	17802	C300.2.5	W225.80	(e)SRW225	-	-	(e)SRW275	SRW300	3	2.4	1.8
	3600	27831	20028	-	W250.80	(e)SRW225	-	-	(e)SRW275	SRW300	3.4	2.8	2.2

that required a larger size than full length SRW profiles. In all cases, a was the longest parameter, followed closely by b. Both areas, a and **b**, worked together to balance the deflections at both side spans. The c length was double, because it was symmetrical on both sides of the supports. It is applicable for intermediate supports of any number of spans, not only for the calculated four-span purlin (33). In the purlin, as a continuous beam, intermediate spans stiffen one another reducing the deflection, thus the c parameter requires a smaller length.

Table 6 analyses the weight of each solution. The weight of steel C-section purlins (C) were taken as a reference, which are compared with the weight of wooden (W) and SRW purlins. Figure 7 shows a graph of the results of those tables. It can be seen that the weights of W and C are similar, except for some cases where the weight of W exceeds the weight of C by up to 45 %. As the characteristics of the profiles are discrete, so too is their behaviour at the design stage, an aspect that García *et al.* (28) also observed. The trend is clear when the SRW profile is used in the whole length: the weight rises in all cases between 15 and 90 %. Nevertheless, the weight of the steel drops between 5 and 38 %. In a few cases the difference was 0 %, *i.e.*, both the SRW and the steel used the same C profile size. In those few cases (4 out of 24), the use of the SRW led to no improvement at all.

The weight of the optimised SRW purlin, in all but three cases, increased between 20 % and 40 % for the C-section purlin. In the three exceptions where the SRW purlin was of reduced weight, the SRW profiles were smaller than the C-section profiles. When comparing the optimised SRW and the wooden purlins, the differences are narrower, the wooden ones being in most cases lighter. The discrete profile size produces jumps, so there was no clear trend. In all cases, the optimised SRW purlins required a smaller profile than wood, which reduced the required quantity of wood between 10 % and 40 % (up to 55 % in two cases). The $a + b + c$ length C-section reinforcements made it possible to reduce the wooden section. These reinforcements also entailed remarkable savings of steel in relation to the C-section purlin, in most cases, above 60 %.

3.3. Sustainability assessment

The impact of the proposed reinforced purlin on the environment has been evaluated in terms of its carbon footprint (29). The carbon footprint per cubic meter of the *Pinus radiata* used in the design of SRW purlin was negative (-781.96

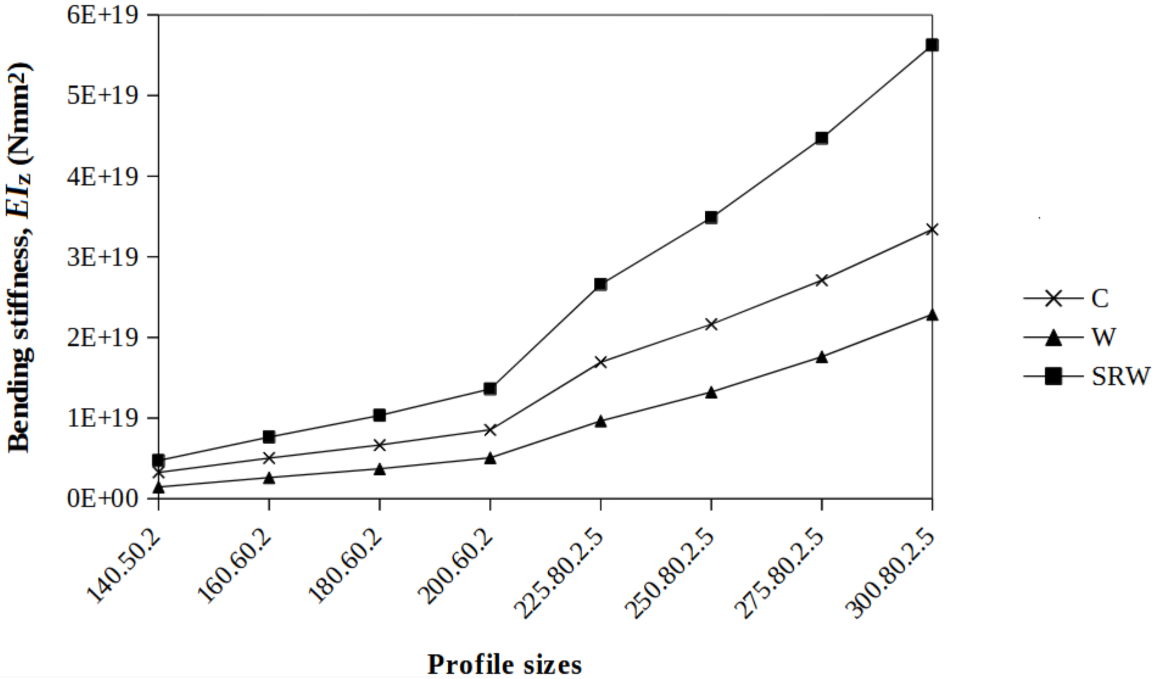

Figure 6: Bending stiffnesses EI_z by profile sizes of wood (W), steel (C), and steel-reinforced wood (SRW).

kg CO_2/m^3) (14). Knowing that its density is 410 kg/m^3, the carbon footprint of one ton of wood is -1.907 Kg CO_2/tn. Steel has a positive carbon footprint of 1.932 kg CO_2/tn (34).

Based on these data, both the carbon footprints of the steel C-section purlin and the optimised SRW purlins were estimated, as compiled in Table 7 and Figure 8. In all the cases under study, the SRW purlins neutralised the carbon footprint of steel, achieving negative values in most cases (almost 5 kg CO_2/kg m). Overall, the longer the span, the larger the reduction of the carbon-footprint.

4. Conclusions

In this study, a new structural typology has been introduced for lightwight roof purlins, where wooden purlins are reinforced with steel C-section profiles within the areas under the highest mechanical stress. In addition, the purlin has been stiffened, thereby reducing any deflection. In this way, this structural element has been released from dependence on steel and its undesirable drawbacks. It opens the door to the use of wood in purlins with high loads and long spans, using acceptable section sizes. Moreover, the new typology also neutralises the carbon footprint of steel purlins, which even becomes negative, providing both a solid and innovative response to the demands of modern society with an eye on the utility of traditional wooden structure. Profile sizes and reinforcement lengths were optimised with analytical calculus and met the requirements of the Spanish technical building code.

In this paper, the analytical approach has been presented as a solid and reliable structural design method, applied in an innovative way. Both engineers and architects can apply this methodology, together with the technical codes and relevant design requirements, to ensure significant improvements to structures and their sustainability. The most remarkable conclusions from this study are as follows:

- The purlin designs of new typology are lighter, which reduce loads and the volume of material needed for the main structure.
- The bending stiffness of the SRW profile (EI_z) is almost double the bending stiffness of the equal-dimensional steel C-section profiles and triple the bending stiffness of the wood. Using only the essential steel to meet the requirements, the wooden profiles are no longer oversized.

Table 6

Comparison of weight in $L = 6.5$ m, 7.5 m and 8.5 m span purlins in comparison with steel C-section purlins.

	Load	Wooden purlin	Entire SRW purlin		Optimised SRW purlin			
	q (N/m)	In comparison with steel $\Delta W_W/W_C$	In comparison with steel $\Delta W_{SRW}/W_C$	Steel saving ΔW_C	In comparison with steel $\Delta W_{SRW}/W_C$	In comparison with wood $\Delta W_{SRW}/W_W$	Steel saving ΔW_C	Wood saving ΔW_W
$L = 6.5$ m	**800**	2.4 %	46.7 %	- 13.1 %	14.2 %	11.5 %	- 67.7 %	- 20.0 %
	1200	44.2 %	70.7 %	- 6.1 %	18.8 %	- 17.6 %	- 67.7 %	- 40.0 %
	1600	35.9 %	75.7 %	- 5.8 %	17.7 %	- 13.3 %	- 63.8 %	- 40.0 %
	2000	- 0.5 %	25.6 %	- 34.1 %	- 10.9 %	- 10.4 %	- 70.6 %	- 40.0 %
	2400	- 0.5 %	25.6 %	- 34.1 %	23.4 %	24.0 %	- 66.2 %	- 10.0 %
	2800	9.4 %	89.5 %	0.0 %	28.0 %	17.0 %	- 61.5 %	- 18.2 %
	3200	9.4 %	89.5 %	0.0 %	35.7 %	24.0 %	- 53.8 %	- 18.2 %
	3600	12.9 %	79.3 %	- 5.4 %	29.5 %	14.7 %	- 64.6 %	- 16.7 %
$L = 7.5$ m	**800**	44 %	70.7 %	- 6.1 %	26.5 %	- 12.3 %	- 69.3 %	- 40.0 %
	1200	- 10 %	15.8 %	- 37.9 %	- 12.6 %	- 2.4 %	- 76.3 %	- 33.3 %
	1600	- 1 %	25.6 %	- 34.1 %	33.4 %	34.1 %	- 62.7 %	- 10.0 %
	2000	9 %	89.5 %	0.0 %	39.4 %	27.4 %	- 56.0 %	- 18.2 %
	2400	13 %	79.3 %	- 5.4 %	28.9 %	14.1 %	- 69.3 %	- 16.7 %
	2800	7 %	70.1 %	- 10.3 %	28.2 %	19.7 %	- 64.6 %	- 16.7 %
	3200	-	70.1 %	- 10.3 %	43.2 %	-	- 56.0 %	-
	3600	-	75.2 %	- 9.8 %	34.0 %	-	- 66.7 %	-
$L = 8.5$ m	**800**	- 10 %	15.8 %	- 37.9 %	- 11.6 %	- 1.3 %	- 75.2 %	- 40.0
	1200	9 %	89.5 %	0.0 %	30.5 %	19.3 %	- 65.9 %	- 50.9 %
	1600	13 %	79.3 %	- 5.4 %	28.5 %	13.8 %	- 62.2 %	- 55.0 %
	2000	- 70.1 %	- 10.3 %	26.4 %	-	- 66.5 %	-	
	2400	-	75.2 %	- 9.8 %	24.2 %	-	- 63.9 %	-
	2800	-	75.2 %	- 9.8 %	29.2 %	-	- 65.3 %	-
	3200	-	-	-	-	-	-	-
	3600	-	-	-	-	-	-	-

Table 7

Carbon footprint of steel C-section and optimised SRW purlins per unit length (kg CO_2/kg m) with respect to the uniformly distributed load, q, and the span length, L.

Load	$L = 6.5$ m		$L = 7.5$ m		$L = 8.5$ m	
q (N/m)	C	SRW	C	SRW	C	SRW
800	9.28	-0.24	9.89	-0.85	15.92	-3.32
1200	9.89	-0.24	15.92	-2.15	15.92	-2.47
1600	10.50	-1.73	15.92	-2.47	16.83	-3.89
2000	15.92	-3.22	15.92	-4.09	17.74	-2.75
2400	15.92	-0.61	16.83	-0.85	18.65	-3.89
2800	15.92	-1.73	17.74	-2.47	18.65	-3.04
3200	15.92	-3.60	17.74	-4.09	-	-4.46
3600	16.83	-0.98	18.65	-1.50	-	-6.18

- The wood-steel combination eliminates the carbon footprint, making it both a feasible and an attractive solution for sustainable construction.
- An analytical calculus method has been used for the optimization of a conventional structural element. As the functions are known, new avenues have been opened up for future implementations of optimization algorithms, which could be used by applying similar criteria to other structural elements.

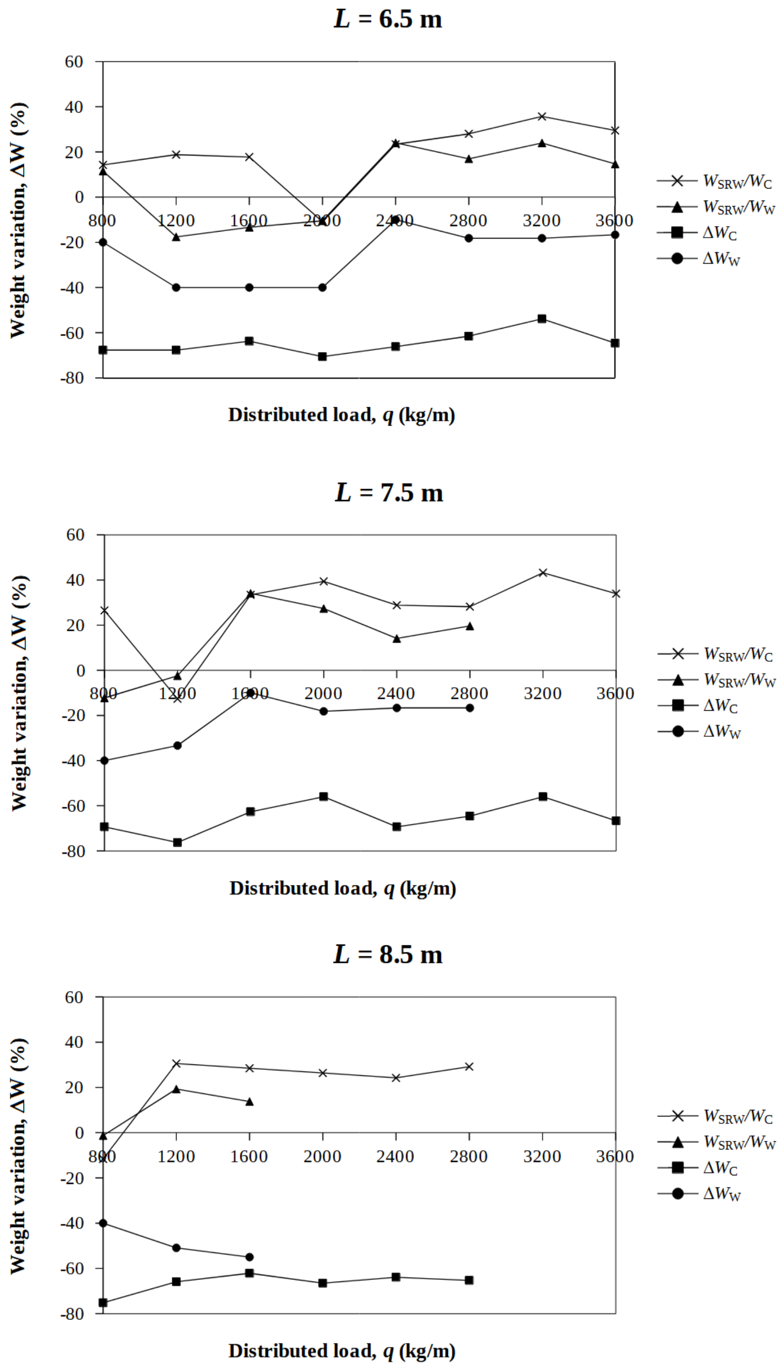

Figure 7: Comparison of optimised SRW with wooden ($\Delta W_{W/SRW}$) and C-section ($\Delta W_{C/SRW}$) purlins; steel (ΔW_C) and wood (ΔW_W) weight savings achieved with the optimised SRW purlin.

Acknowledgements

The authors wish to express their gratitude to the Provincial Council of Gipuzkoa through Etorkizuna Eraikiz agreement and to the SAREN research group (IT1619-22, Basque Government).

Open Access funding provided by University of Basque Country UPV/EHU.

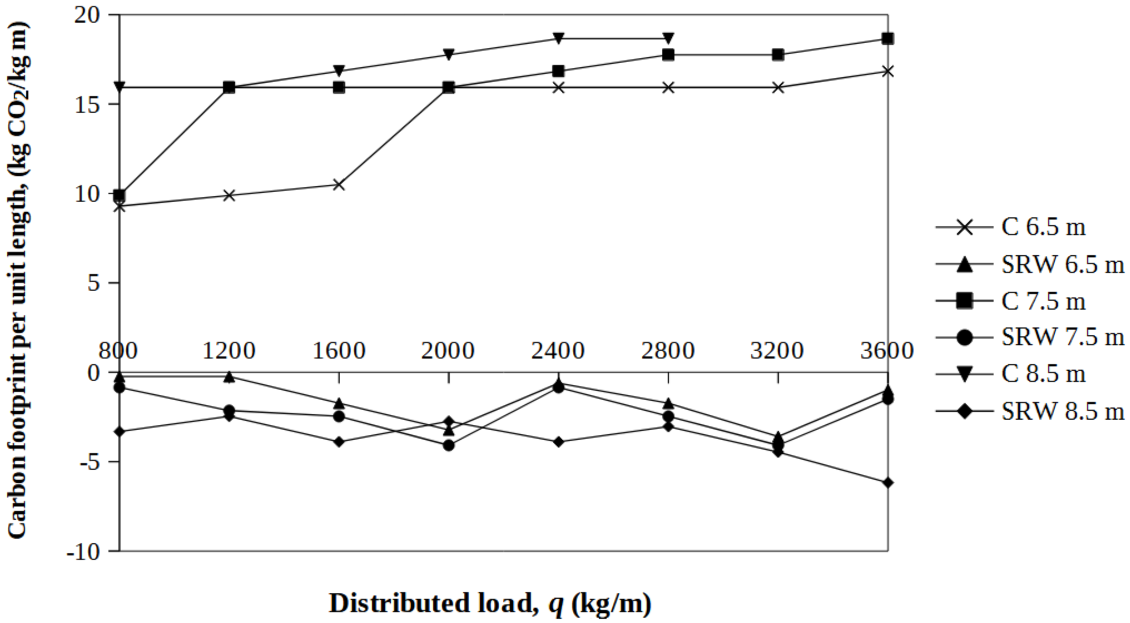

Figure 8: Carbon footprint of steel C-section and optimised SRW purlins per unit length.

References

[1] V. J. Gan, C. M. Chan, K. Tse, I. M. Lo, J. C. Cheng, A comparative analysis of embodied carbon in high-rise buildings regarding different design parameters, Journal of Cleaner Production 161 (2017) 663–675.

[2] B. Upton, R. Miner, M. Spinney, L. S. Heath, The greenhouse gas and energy impacts of using wood instead of alternatives in residential construction in the united states, Biomass and Bioenergy 32 (1) (2008) 1–10.

[3] S. Li, H. Wu, Z. Ding, Identifying sustainable wood sources for the construction industry: a case study, Sustainability 10 (1) (2018) 139.

[4] A. Hafner, How building with wood can be linked to sales of building plots: Results from an exemplary site development in munich, germany, Sustainability 9 (6) (2017) 947.

[5] M. C. Caruso, C. Menna, D. Asprone, A. Prota, G. Manfredi, Methodology for life-cycle sustainability assessment of building structures, ACI Structural Journal 114 (2) (2017) 323.

[6] A. Padilla-Rivera, B. Amor, P. Blanchet, Evaluating the link between low carbon reductions strategies and its performance in the context of climate change: a carbon footprint of a wood-frame residential building in quebec, canada, Sustainability 10 (8) (2018) 2715.

[7] J. Švajlenka, M. Kozlovská, Perception of user criteria in the context of sustainability of modern methods of construction based on wood, Sustainability 10 (2) (2018) 116.

[8] X. Zhang, M. Shahnewaz, T. Tannert, Seismic reliability analysis of a timber steel hybrid system, Engineering Structures 167 (2018) 629–638.

[9] A. K. B. Marsono, A. T. Balasbaneh, Combinations of building construction material for residential building for the global warming mitigation for malaysia, Construction and Building Materials 85 (2015) 100–108.

[10] L. Wang, A. Toppinen, H. Juslin, Use of wood in green building: a study of expert perspectives from the uk, Journal of cleaner production 65 (2014) 350–361.

[11] A. Stocchero, J. K. Seadon, R. Falshaw, M. Edwards, Urban equilibrium for sustainable cities and the contribution of timber buildings to balance urban carbon emissions: A new zealand case study, Journal of cleaner production 143 (2017) 1001–1010.

[12] A. Haapio, P. Viitaniemi, A critical review of building environmental assessment tools, Environmental impact assessment review 28 (7) (2008) 469–482.

[13] A. Woodard, H. Milner, Sustainability of timber and wood in construction, in: Sustainability of construction materials, Elsevier, 2016, pp. 129–157.

[14] A. H. Buchanan, S. John, S. Love, et al., Life cycle assessment and carbon footprint of multi-storey timber buildings compared with steel and concrete buildings/by andrew buchanan, stephen john and simon love (2013).

[15] J. E. Jakes, X. Arzola, R. Bergman, P. Ciesielski, C. G. Hunt, N. Rahbar, M. Tshabalala, A. C. Wiedenhoeft, S. L. Zelinka, Not just lumber—using wood in the sustainable future of materials, chemicals, and fuels, Jom 68 (9) (2016) 2395–2404.

[16] J. Perez-Garcia, B. Lippke, D. Briggs, J. B. Wilson, J. Bowyer, J. Meil, The environmental performance of renewable building materials in the context of residential construction, Wood and Fiber Science 37 (2005) 3–17.

[17] R. Ward, Tackle Climate Change, Use Wood, BC Forestry Climate Change Working Group, Victoria (Canada) (2009).

[18] J. Canto-Perello, M. P. Martinez-Garcia, J. Curiel-Esparza, M. Martin-Utrillas, Implementing sustainability criteria for selecting a roof assembly typology in medium span buildings, Sustainability 7 (6) (2015) 6854–6871.

[19] P. Dietsch, Robustness of large-span timber roof structures—structural aspects, Engineering Structures 33 (11) (2011) 3106–3112.
[20] C. H. Pham, G. J. Hancock, Direct strength design of cold-formed purlins, Journal of Structural Engineering 135 (3) (2009) 229–238.
[21] Y. O. Özkılıç, C. Aksoylu, M. H. Arslan, Experimental and numerical investigations of steel fiber reinforced concrete dapped-end purlins, Journal of Building Engineering 36 (2021) 102119.
[22] O. A. Hegeir, T. Kvande, H. Stamatopoulos, R. A. Bohne, Comparative life cycle analysis of timber, steel and reinforced concrete portal frames: A theoretical study on a norwegian industrial building, Buildings 12 (5) (2022) 573.
[23] Código técnico de la edificación: Seguridad estructural CTE-DB-SE, Ministerio de Fomento, Real Decreto 314/2006 314 (2006).
[24] A. S. Sayyad, Y. M. Ghugal, Bending, buckling and free vibration of laminated composite and sandwich beams: A critical review of literature, Composite Structures 171 (2017) 486–504.
[25] S. M.-E. Sacco, Computational modeling of FRP reinforced cementitious beams, Mechanics of Advanced Materials and Structures 13 (4) (2006) 339–353.
[26] C. Timbolmas, R. Bravo, F. J. Rescalvo, M. Portela, Transformed-section method applied to multispecies glulam timber beams subjected to pure bending, Mechanics of Advanced Materials and Structures 29 (27) (2022) 6814–6823.
[27] F. J. Rescalvo, C. Timbolmas, R. Bravo, M. Portela, J. Lorenzana, Multi-side digital image correlation (DIC) evaluation of CFRP bonded to poplar timber, Mechanics of Advanced Materials and Structures (2023) 1–10.
[28] H. García, M. Zubizarreta, J. Cuadrado, J. L. Osa, Sustainability improvement in the design of lightweight roofs: A new prototype of hybrid steel and wood purlins, Sustainability 11 (1) (2018) 39.
[29] J. Cuadrado, M. Zubizarreta, B. Pelaz, I. Marcos, Methodology to assess the environmental sustainability of timber structures, Construction and Building Materials 86 (2015) 149–158.
[30] ACCESS-STEEL SS053-proyecto básico: Diseño de estructura de correas, ASCEM, Madrid (2012).
[31] B. J. Goodno, J. M. Gere, Mechanics of materials, Cengage learning, 2020.
[32] UNE 36573:1979 productos de acero. perfiles abiertos conformados en frío. perfil CF. medidas (1979).
[33] R. Nonnast, El proyectista de estructuras metálicas, Paraninfo, 1987.
[34] H. Freeman, L. Christie, Reducing the whole life carbon impact of buildings, POSTbrief (Parliamentary Office Of Science and Technology) (43) (2021).